An Experimental Study on Laser Ablation of Ultra-thin SiN_x Layer of PERC Solar Cell

WCMNM 2021

Pinal Rana[1], Durga Prasad Khatri[2,3], Anil Kottantharayil[2,3], Deepak Marla[1]

[1]Department of Mechanical Engineering
[2]Department of Electrical Engineering
[3]National Centre for Photovoltaics Research and Education
Indian Institute of Technology Bombay

Abstract

In this work, a nanosecond green laser (532 nm) is used to generate narrow openings by removing an ultra-thin (~85 nm) SiN_x layer that is coated on a silicon substrate for application in the fabrication of Passivated Emitter and Rear Contact (PERC) solar cells. An experimental analysis is presented to identify the optimal range of laser parameters for an efficient ablation with minimal damage to the silicon substrate. The ablated samples were characterized using a 3D profilometer to obtain the surface profiles, scanning electron microscope imaging to observe the surface quality, and energy-dispersive X-Ray line scan to evaluate the nitrogen content. The experimental results suggest that the SiN_x layer starts to ablate only above a threshold laser fluence of 1.4 J/cm^2, while the surface bulged out for laser fluence slightly below the ablation threshold. The nitrogen content was the lowest for a surface processed at 2.4 J/cm^2 of laser fluence value. The central part of the ablated region was clean with a negligible concentration of nitrogen, suggesting complete ablation of the SiN_x layer for establishing electrical contacts. The ablation width was close to the laser spot diameter only at lower values of the laser fluence. The lowest value of ablation depth was about 180 nm, suggesting that only about 95 nm layer of the silicon is ablated. The study demonstrates that nanosecond laser ablation is a potential technique for ablation of the SiN_x layer of PERC solar cells but requires choosing the optimal parameters.

Keywords: Nanosecond laser, Passivation layer, Laser ablation, PERC solar cell

1. Introduction

The Passivated Emitter and Rear Cell or Passivated Emitter and Rear Contact (PERC) solar cells are modified conventional silicon-based solar cells with 6-8 % higher efficiency [1]. PERC solar cell contains 85-100 nm thin passivation layer of a dielectric material such as SiN_x, SiO_2, SiO_xN_y, or Al_2O_3 [2] on the rear side. In order to create electrical contacts with the silicon wafer, narrow openings are created by selectively removing the passivation layer. Various techniques such as photolithography [3], diamond scratching [4], and laser ablation [5] have been reported in the literature to create narrow openings. The main challenge here is to remove the passivation layer locally with minimal damage to the underlying silicon substrate. Laser ablation processes are very fast, stable, cost-effective, and reliable over other methods.

Laser ablation is commonly performed using pulsed lasers with pulse durations in the range of nanoseconds (ns), picoseconds (ps), and femtoseconds (fs) [6,7]. Experimental work of Chiu et al. [8] successfully demonstrated the use of a nanosecond laser (532 nm wavelength) for ablation of SiN_x layer of PERC solar cell. Experimental investigation using a picosecond laser to ablate a SiN_x layer deposited on a silicon substrate were carried out by Heinrich et al. [9] at three different wavelengths corresponding to the UV, visible, and IR regime. The authors observed that the ablation mechanisms differed with laser wavelength as the absorption in the SiN_x layer is strongly wavelength-dependent. Besides, all the wavelengths seem to influence the crystalline structure of the ablated surface due to recrystallization and amorphization. They concluded that picosecond lasers with wavelength only in the UV regime can effectively ablate the SiN_x layer for applications in solar cells. Experimental investigations of Zeng et al. [10] on laser ablation of silicon using UV nanosecond and UV femtosecond lasers show that the ablation efficiency is superior in the case of femtosecond lasers. The ablation crater produced using a femtosecond laser was twice deeper than that obtained using a nanosecond laser. This was attributed to the higher intensities in the femtosecond laser and enhanced plasma shielding effects in the nanosecond laser. Besides, a large amount of material deposition at the crater's edge was observed in nanosecond laser processing. However, experimental studies of Ali et al. [11] on laser ablation of SiN_x layer of PERC solar cells reveal that the electrical performance of PERC solar cells fabricated using nanosecond laser processing is superior than femtosecond laser processing. The authors did a comparative study on the laser ablation of the passivation layer using nanosecond and femtosecond laser at green wavelengths. They observed that femtosecond laser processing induces severe damages in the silicon substrate, causing a reduction in solar cell performance. Therefore, it is evident from the literature that nanosecond lasers can be used to ablate the thin passivation layers of PERC solar cells. However, the poor ablation characteristics produced using the nanosecond lasers severely limit their usage. Hence the need to optimize the nanosecond laser parameters to enhance the ablation characteristics is critical to their application in the field of the solar cell.

In this work, nanosecond laser ablation of SiN_x layer of thickness ~85 nm deposited on a silicon substrate is studied experimentally to understand the effect of process parameters on the ablated surface characteristics with an aim to identify the optimal range of laser parameters to be used. Experiments are carried out over a range of laser parameters, and the ablated surface was analysed using optical scan profilometry, scanning electron microscope (SEM) imaging, and energy-dispersive X-ray (EDX) technique.

2. Experiments

The samples consist of a 280 μm thick p-type silicon substrate (of 3 Ω-cm resistivity) with a thin layer of SiN_x deposited on it using plasma-enhanced chemical vapor deposition (PECVD). The thickness of the SiN_x layer was measured using ellipsometry and found to be 85 nm (refer Fig.1) with refractive index of 2.01 and extinction coefficient is nearly zero at 532 nm wavelength. Ablation experiments were carried out using a nanosecond green laser system, SLTL Scribo, manufactured by SLTL, India. The laser system consists of a solid-state $NdYVO_4$ laser source emitting pulses of duration 25 ns in TEM_{00} mode at a wavelength of 532 nm. The laser pulse repetition rate (PRR) can be varied between 1 kHz to 150 kHz, and the average laser power can be varied between 0.05-30 W by adjusting the current. The laser is focussed using a planoconvex lens of focal length 70 mm, generating a spot diameter of 25 μm, corresponding to the $1/e^2$ profile. Laser scanning is achieved by the movement of a CNC XYZ stage on which the samples are mounted.

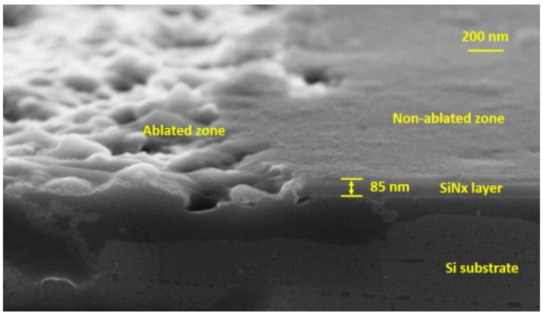

Figure 1 Cross-sectional SEM images of the SiNx coated Silicon sample

Based on a preliminary study, it was observed that ablation characteristics were good only when the laser fluence was between 1.5 – 7.8 J/cm^2. Above 7.8 J/cm^2 very high ablation occurred resulting in poor surface characteristics, while no ablation occurred below 1.5 J/cm^2 laser fluence. Further, experiments were carried to understand the effect of laser fluence, which was controlled by changing average laser power and PRR. The average laser power was varied between 0.06 W to 0.52 W. This was achieved by changing the current in the system between 8 A to 9.25 A. Further, PRR were chosen between 40 – 50 kHz and calculated value of laser fluence. During all the experimentation a fixed value of the scanning speed is chosen which is equal to 1 m/min. All the other parameters such as spot diameter, pulse duration, and wavelength were kept fixed.

The ablated samples were analyzed using three different characterization techniques. An optical microscope (Alicona infinite focus G5) was used to measure the surface profile of the ablated samples. The data of depth and width of the ablated region was obtained from the surface profiles. High-resolution images of the ablated samples were also obtained using a SEM (Zeiss Ultra 55) to observe the surface characteristics. In order to verify if the ablation was clean, nitrogen content on the samples was measured using the EDX technique on Zeiss Ultra 55 machine. The nitrogen content was measured by a line scan along the width of the ablated region.

3. Results and discussion

3.1 Surface characteristics

Figure 2 (a) shows an SEM image of a laser-ablated sample at a laser fluence of 2.4 J/cm^2. Change in color and texture of the surface due to ablation is evident. High magnification images of the edge and central part of the ablated region shown in Figs. 2(b) and 2(c), respectively, give a clear picture of the surface. The edges are seen to contain a large number of pores, while the central part has a relatively smoother surface in comparison.

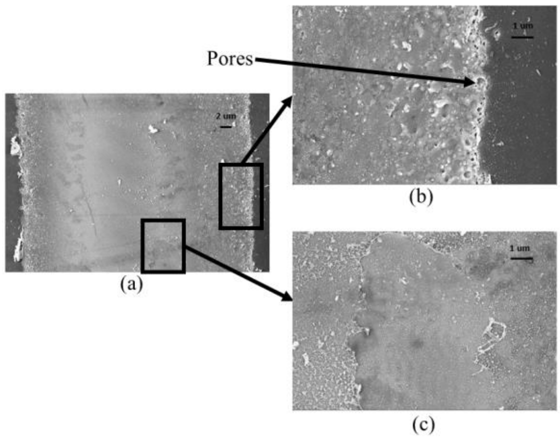

Figure 2 Surface image of the sample at 2.4 J/cm2.

The shape of the surface profile for the sample in Fig. 2 is shown in Fig. 3, represented by the line corresponding to 2.4 J/cm^2. Note that the scales on the x and y axes are different. The surface profile suggests that the maximum ablation depth of ~ 315 nm is observed at the center and decreases along the width. Humps are formed at the edges, possibly due to the solidification of molten material driven out by

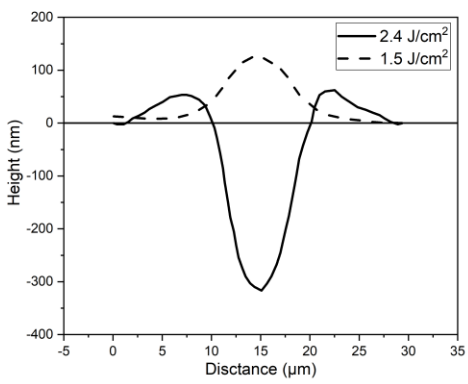

Figure 3 Crater profile of two different process parameters namely 1.5 and 2.4 J/cm^2.

Marangoni convection and vapor pressure exerted by the ablated material [12].

The ablated samples were observed to have a distinct surface below a particular threshold value of the laser fluence. The surface profile in Fig. 3 represented by a dotted line corresponds to a lower laser fluence of 1.5 J/cm^2. Unlike the one at 2.4 J/cm^2 of laser fluence, the surface profile at 1.5 J/cm^2 laser fluence does not have any ablation depth (or material removal). The surface appears to have bulged out. This is an interesting phenomenon that sheds light on the mechanism involved in the ablation process. The bulging effect could be due to the heating of the material below the normal boiling point and its subsequent expansion due to thermal effects. Due to high temperature, the material undergoes plastic deformation, and upon cooling, retains the shape. The deformation of the material is most likely to occur due to the sub-surface heating effect. Since the SiN_x layer is transparent to the laser radiation, it does not absorb any radiation. Laser radiation absorption occurs only in the silicon layer. Subsequently, the SiN_x layer also gets heated up due to conduction of heat from the underlying silicon layer. Therefore, the temperature is maximum at the interface and gradually decreases outward in the SiN_x layer, with the top surface having the lowest temperature. At lower laser fluence, it is likely that the temperature of the top part of the SiN_x layer does not reach the normal boiling point for ablation to initiate. However, the sub-surface region could be at much higher temperatures, leading to bulging of the material. A schematic representation of this phenomenon is shown in Fig. 4.

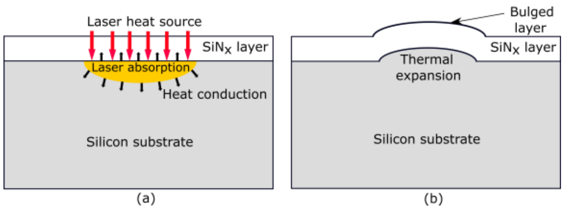

Figure 4 Bulged layer formation mechanism in SiN_x coated silicon substrate.

3.2 Ablation depth and width

The variation in ablation width and depth with laser fluence are shown in Figs 5 and 6, respectively. The measurements were taken at three different locations in the ablated region, and the average value is reported. It can be observed that, no ablation occurs below 1.5 J/cm^2 laser fluence. Further, the data also suggests that with an increase in laser fluence ablation width is increases. This is because the heat input per unit area increases with an increase in laser fluence and ablation of the material largely depends on the laser fluence or pulse energy. No ablation occurs if the laser fluence is below a specific threshold value, as observed for the 0.9 J/cm^2 values of the laser fluence.

The trends in ablation width and depth are similar. The increase in ablation width and depth with an increase in the laser fluence is very significant initially up to laser fluence of 3.9 J/cm^2. Beyond this value of the laser fluence, increase in ablation depth and width is marginal. This could be due to the effect of plasma

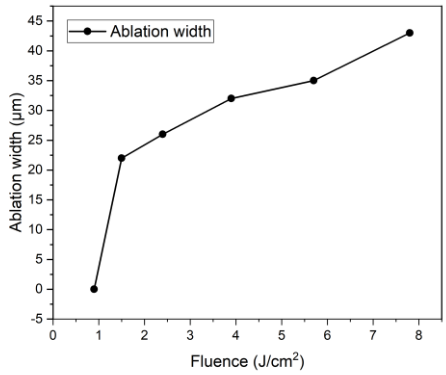

Figure 5 Variation in ablation width with laser fluence.

shielding, which becomes significant at higher laser fluences, leading to saturation in ablation depth. A similar trend has been predicted using a computation model by Marla et al. [13]. The ablation width in Fig. 5 is lower than the spot size of 25 µm only at lower laser fluence values. At higher laser fluence, the ablation width is nearly double that of the spot size. Besides, an ablation depth of less than 190 nm is observed only for 1.5 J/cm^2 laser fluence. At all other values, the ablation depth is more than 230 nm. A higher value of ablation depth is undesirable as it increases the losses due to surface recombination. Therefore, the experiments reveal that lower laser fluence are preferable for precise ablation.

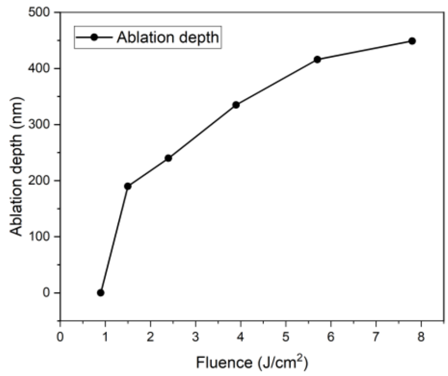

Figure 6 Variation in ablation depth with laser fluence.

3.3 Nitrogen content

The nitrogen content in the ablated region plays a vital role in solar cell performance. If the SiN_x layer is not adequately ablated, the printed aluminum paste may not make proper electrical contact with the silicon beneath owing to its insulation property. This may lead to higher surface recombination losses and reduces the performance of the PERC solar cell. Figure 7 shows a plot of nitrogen content at 2.4 J/cm^2 laser fluence measured along the width of the ablation channel using EDX. Measurements are taken both in the ablated as well as non-ablated region to have a comparison between the two. The amount of nitrogen content in the ablated region is as low as 0.76 counts, whereas the count is 3.29 in the non-ablated region. During the laser ablation process, when the temperature of SiN_x reaches 2150 K, it decomposes into silicon and nitrogen [14]. Ideally, nitrogen content in the ablated region should be zero. However, traces of nitrogen can be present due to: (i) chemical reaction with ambient air as the silicon material reaches higher temperatures during the ablation, and (ii) due to the decomposition of SiN_x layer into silicon and nitrogen, and subsequent diffusion of nitrogen into the underlying silicon.

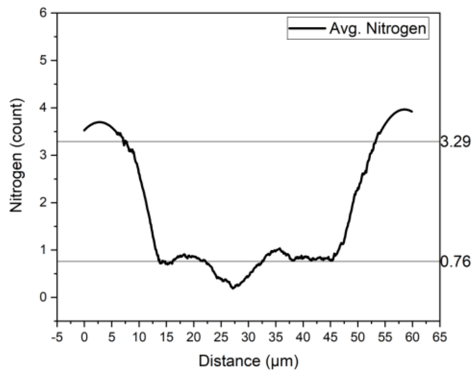

Figure 7 Variation in nitrogen content in the ablated and non-ablated region at 2.4 J/cm^2 laser fluence

The ratio of nitrogen content in the ablation region to the non-ablated region can be used to analyze the quality of ablation. If the ratio is close to zero, it can be considered as an efficient ablation process. Figure 8 shows the variation in the ratio of nitrogen content with laser fluence. With an increase in laser fluence, the ratio has a steep decline initially and then shows a marginal decrease after that. A sudden drop from 1 to 0.076 when the laser fluence is increased from 1 J/cm^2 to 2.4 J/cm^2 signifies the onset of ablation. With an increase in the laser fluence, the ratio is seen to increase, which could be due to the reasons outlined above. This data suggests that moderate values of laser fluence are preferred for an efficient ablation.

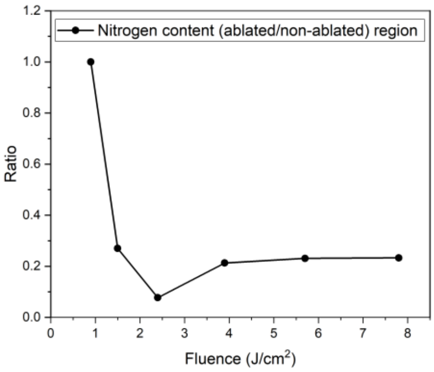

Figure 8 Ratio of nitrogen content in ablated and non-ablated region with laser fluence.

4. Conclusions

Localized removal of the thin (~85 nm) SiN_x layer of PERC solar cells is essential in establishing electrical contact. This work demonstrates the use of a green nanosecond laser for localized ablation of the SiN_x layer. Based on the surface profile and SEM images of the ablated area at different laser fluence, this study found that subsurface heating precedes the ablation. This was identified to occur due to the transparent nature of the SiN_x layer, causing laser absorption only in the underlying silicon. As a consequence, bulging on the SiNx layer occurs at lower laser fluence due to thermal deformation or decomposition at the silicon-SiN_x interface. The ablated surface was clean at the central part, while the edges had humps with pores. Ablation width and depth were found to increase with an increase in laser fluence. Lower laser fluence were identified to produce precise ablation with moderate width and minimal depth. However, the nitrogen content in the ablated region was found to be minimal at moderate values of laser fluence. The experimental study established that green nanosecond lasers can be used for efficient removal of the SiN_x layer of PERC solar cells. The optimal values of laser parameters were identified as 2.4 J/cm^2 laser fluence.

Acknowledgments

This work was supported by the National Centre for Photovoltaic Research and Education (NCPRE) and IIT Bombay. NCPRE is funded by the Ministry of New and Renewable Energy (MNRE), Government of India. The authors thank Saima Cherukat for her support during analysis and characterization.

References

[1] Saga T. Advances in crystalline silicon solar cell technology for industrial mass production. npg asia materials. 2010 Jul;2(3):96-102.
[2] N Balaji et al., Electrical and optical characterization of SiOxNy and SiO2 dielectric layers and rear surface passivation by using SiO2/SiOxNy stack layers with screen printed local Al-BSF for c-Si solar cells. *Current Applied Physics*, 2018 *18*(1), pp.107-113.
[3] A Spott et al., Photolithographic fabrication of slot waveguides. In Advanced Fabrication Technologies for Micro/Nano Optics and Photonics IV, 2011 volume 7927, page 792704.
[4] Z Zhang Z et al. Changes in surface layer of silicon wafers from diamond scratching. Cirp Annals. 2015 Jan 1;64(1):349-52.
[5] A Blakers. Development of the perc solar cell. IEEE Journal of Photovoltaics, 2019, 9(3):629–635.
[6] D Walter et al., Damage free ultraviolet nanosecond laser ablation for high efficiency back contact solar cell fabrication. Solar Energy Materials and Solar Cells, 2015, 136:1–10.
[7] M Kim et al., Analysis of laser-induced damage during laser ablation process using picosecond pulse width laser to fabricate highly efficient perc cells. Solar Energy, 2014, 108:101–106.
[8] J S Chiu et al., The role of laser ablated backside contact pattern in efficiency improvement of mono crystalline silicon PERC solar cells. Solar Energy, 2020, 196, pp.462-467.
[9] G Heinrich et al., Investigation of ablation mechanisms for selective laser ablation of silicon nitride layers. Energy Procedia. 2011 Jan 1;8:592-7.
[10] X Zeng et al., Experimental investigation of ablation efficiency and plasma expansion during femtosecond and nanosecond laser ablation of silicon. Applied Physics A. 2005 Feb;80(2):237-41.
[11] J M Ali et al., Analysis of nanosecond and femtosecond laser ablation of rear dielectrics of silicon wafer solar cells. Solar Energy Materials and Solar Cells, 2019, 192:117–122.
[12] M V Shugaev et al., Laser-induced thermal processes: Heat transfer, generation of stresses, melting and solidification, vaporization and phase

explosion. Handbook of Laser Micro-and Nano-Engineering, 2020.
[13] D Marla et al., Transient Analysis of Laser Ablation Process with Plasma Shielding: One Dimensional Model using Finite Volume Method. Journal of Micro and Nano-Manufacturing, 2013, 1:011007.
[14] G Poulain et al., Modeling of laser processing for advanced silicon solar cells. In Excerpt from the Proceedings of the COMSOL Conference, 2010.